

# Grid Tied Independent Mppt Control For Each Module With Q-Zsource Cascaded 11-Level Inverter

*1.Kommu Manoj Kumar, PG Student, 2.C.Balachandra Reddy, Professor & HOD  
Department of EEE, CBTVIT, Hyderabad*

**Abstract**—The quasi-Z source (qZS) cascaded multilevel inverter (qZS-CMI) presents attractive advantages in application to photovoltaic (PV) power system. Each PV panel connects to a qZS H-bridge inverter (qZSI) to form a power generation module. The distributed maximum power point tracking (MPPT) and all modules' dc-link peak voltage balance can be achieved. However, it is the same to the conventional CMI that the 2nd harmonic (2w) voltage and current ripples exist in each qZSI module. It is crucial for a qZS-CMI to design the reasonable qZS network parameters to limit the ripples within a desired range. This paper proposes an analytic model to accurately calculate the 2w voltage and current ripples of each qZSI module. An qZS impedance design method based on the built model is proposed to limit the 2w ripples of dc-link voltage and inductor current. Simulated and experimental results through using the designed 1.5-kW prototype validate the proposed analytic model and the design method. Furthermore, this paper analyzes all of the operating states for an qZSI module and calculates the power loss. The measured efficiency from the prototype verifies the theoretical calculation, and the qZS-CMI based grid-tie PV power system is tested in practical.

**Index Terms**— Circuit modeling, multilevel inverter, photovoltaic power generation, quasi-Z source inverter.

## I. INTRODUCTION

The photovoltaic (PV) power era turning out to be more prominent, the applications and examines of multilevel inverter based PV power frameworks are developing consistently because of multilevel inverters' focal points and substantial force scale/high voltage lattice tie requests. cascaded multilevel inverter (CMI) [1]–[6] has remarkable favorable circumstances in connected to the PV power framework, in light of the fact that it can accomplish the circulated most extreme force point following (MPPT) to increment the framework productivity, and accomplish high-voltage/high power framework tie without transformer. Be that as it may, in the ordinary CMI based PV power framework, every module is a buck inverter, furthermore, its dc-join voltage changes alongside the PV board voltage. So when the MPPT is utilized in every module, the uneven dc-join voltage will happen between all modules.

Z/quasi-Z-source cascaded multilevel inverters (ZS/qZSCMIs) overcome above disservices of ordinary CMI through consolidating ZS/qZS system and H-span module together [7]–[11], due to the ZS/qZS inverter's (ZSI/qZSI) buck/ help and reversal in a solitary stage [12]–[19].

The 2nd consonant (2w) voltage and current swells dependably exist in every module of CMI. A colossal dc-join capacitor is needed in every H-span module of conventional CMI to breaking point the voltage swell. So also, the ZS/qZS-CMI additionally has the 2w voltage and current swells in every ZS/qZSI module. Some writings concentrate on investigating and dispensing with low recurrence swells of every capacitor voltage and inductor current [8], [15], [16]. An air conditioner proportionate model is assembled to examine the 2w swells of the qZSI module in [8], yet the manufactured model contains five comparisons, where the coupled relationship makes the examination also, plan troublesome, and there is no test confirmation.

The low recurrence symphonious end PWM is proposed in [15] through investigating the relationship of 2w voltage and current swells with ZS capacitance, inductance, shoot-through obligation proportion, and tweak file, yet the got mathematical statements are excessively perplexing for ZS system outline. Two smoothing-force circuits are utilized in [16] to decrease the 2w swell of dc-connection top voltage in single-stage ZSI, however the extra circuits expand the framework expense and many-sided quality. New research advancement is coveted on building exact 2w swell investigative model and the point by point plan strategy for the capacitance and inductance for ZSI/qZSI module.

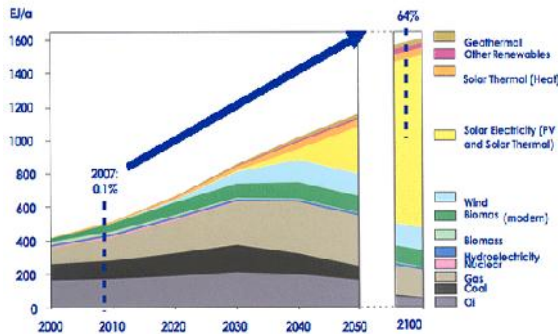
For customary H-span module in CMI, there are two working states, i.e., dynamic state and zero state. While, for ZS/qZS-CMI, working states are tiny bit complex as a result of extra shoot-through states when ascertaining inverter proficiency. In [8], the creators dissect the qZSI module proficiency, yet the qZS system diode's misfortune count did not incorporate the opposite recuperation misfortune, and the conduction misfortune overlooked the resistance misfortune, which will certainly influence the figured effectiveness. Up to now, there is no writing to dissect the equal circuits of ZSI/qZSI module to clear up all working states, and there is no writing to present the ZS/qZS-CMI gadget conduction current with the precise time interim, which are identified with precisely appraise the misfortune.

This paper proposes an exact 2w cascaded model, and the qZS impedance outline and the nitty gritty proficiency examination for the qZS-CMI are tended to. The model is assembled to check the proposed model and proficiency investigation. The qZS-CMI based PV power framework is tried in handy, and the circulated MPPT control, the adjusted dc-connection top voltage, and the PV power matrix tie a

### 1.1 How electricity is generated through solar power:

With the worsening of the world's energy shortage and environmental pollution problems, protecting the energy and the environment becomes the major

problems for human beings. Thus the development and application of clean renewable energy, such as solar, wind, fuel cell, tides and geothermal heat etc., are getting more and more attention. Among them, solar power will be dominant because of its availability and reliability. As predicted by [1], the solar will provide the electricity up to 64% of the total energy by the end of this century as shown in below Figure.



Photovoltaic (PV) power generation has become one of the main ways to use solar energy. And the renewable energy source based distributed generation (DG) system are normally interfaced to the grid through power electronic converters or inverters [2] as shown in Figure 1.2. Thus developing a photovoltaic grid-connected inverter system is important for the mitigation of energy and environmental issues.

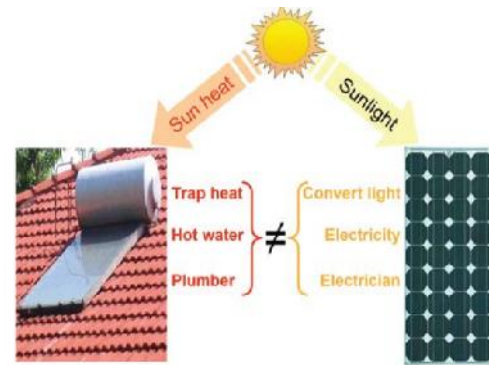
II. LITERATURE SURVEY  
**STRUCTURE OF THE PV SYSTEM**

A photovoltaic system, also photovoltaic power system, solar PV system, PV system or casually solar array, is a power designed to supply usable solar power by means of photovoltaic. It consists of an arrangement of several components, including solar panels to absorb and directly convert sunlight into electricity, a solar inverter to change the electrical current from DC to AC, as well as mounting, cabling and other electrical accessories to set-up a working system. It may also use a solar tracking system to improve the system's overall performance or include an integrated battery solution, as prices for storage devices are expected to decline. Strictly speaking, a solar array only encompasses the ensemble of solar panels, the visible part of the PV system, and does not include all the other hardware, often summarized as balance of system (BOS). Moreover, PV systems convert light directly into electricity and shouldn't be confused with other solar technologies, such as concentrated solar power (CSP) and solar thermal, used for both, heating and cooling.

PV systems range from small, roof-top mounted or building-integrated systems with capacities from a few to several tens of kilowatts, to large utility-scale power stations of hundreds of megawatts. Nowadays, most PV systems are connected to the electrical grid, while stand-alone or off-grid systems only account for a small portion of the market.

Operating silently and without any moving parts or environmental emissions, PV systems have developed into a mature technology that has been used for fifty years in specialized applications, and grid-connected systems have been operating for over twenty years. A roof-top system recoups the invested energy for its manufacturing and installation within 0.7 to 2 years and produces about 95 percent of net clean renewable energy over a 30-year service lifetime.

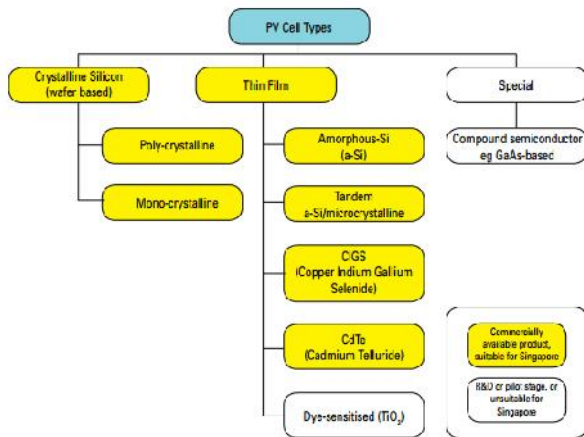
As the growth of photovoltaic fits an exponential curve, prices for PV systems have rapidly declined in recent years. However, they vary by market and the size of the system. In 2014, prices for residential 5kW-systems in the United States were around \$3.29 per watt, while in the highly penetrated German market, prices for rooftop systems of up to 100 kW declined to €1.24 per watt. Nowadays, solar PV modules account for less than half of the system's overall cost leaving the rest to the remaining BOS-components and to soft costs, which include customer acquisition, permitting, inspection and interconnection, installation labor and financing costs.



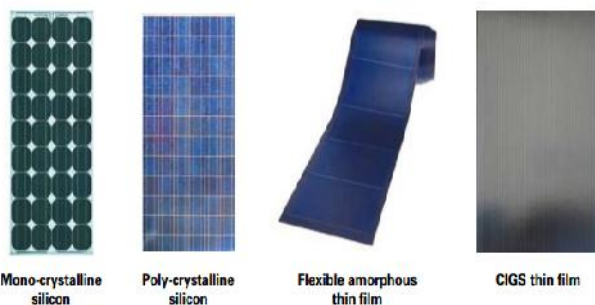
The difference between solar thermal and solar PV systems

**Solar PV Technology**

A solar PV system is powered by many crystalline or thin film PV modules. Individual PV cells are interconnected to form a PV module. This takes the form of a panel for easy installation. PV cells are made of light-sensitive semiconductor materials that use photons to dislodge electrons to drive an electric current. There are two broad categories of technology used for PV cells, namely, crystalline silicon, as shown in Figure 4 which accounts for the majority of PV cell production; and thin film, which is newer and growing in popularity. The "family tree" in Figure 5 gives an overview of these technologies available today and Figure 6 illustrates some of these technologies.



PV technology family tree



Common PV module technologies

**Crystalline Silicon and Thin Film Technologies**

Crystalline cells are made from ultra-pure silicon raw material such as those used in semiconductor chips. They use silicon wafers that are typically 150-200 microns (one fifth of a millimeter) thick. Thin film is made by depositing layers of semiconductor material barely 0.3 to 2 micrometers thick onto glass or stainless steel substrates. As the semiconductor layers are so thin, the costs of raw material are much lower than the capital equipment and processing costs.

**Conversion Efficiency:**

Technology	Module Efficiency
Mono-crystalline Silicon	12.5-15%
Poly-crystalline Silicon	11-14%
Copper Indium Gallium Selenide (CIGS)	10-13%
Cadmium Telluride (CdTe)	9-12%
Amorphous Silicon (a-Si)	5-7%

Apart from aesthetic differences, the most obvious difference amongst PV cell technologies is in its conversion efficiency, as summarized in Table 1. For example, a thin film amorphous silicon PV array will need close to twice the space of a crystalline silicon PV array because its module efficiency is halved, for the same nominal capacity under Standard Test Conditions1 (STC)

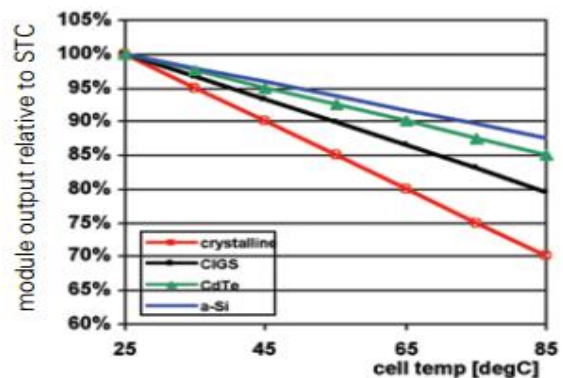
rating. For crystalline silicon PV modules, the module efficiency is lower compared to the sum of the component cell efficiency due to the presence of gaps between the cells and the border around the circuit i.e., wasted space that does not generate any power hence lower total efficiency.

**Effects of Temperature**

Another important differentiator in solar PV performance, especially in hot climates, is the temperature coefficient of power. PV cell performance declines as cell temperature rises. For example, in bright sunlight, cell temperatures in Singapore can reach over 70°C, whereas PV modules are rated at a cell temperature of 25°C. The loss in power output at 70°C is therefore measured as (70 - 25) x temperature coefficient. Most thin film technologies have a lower negative temperature coefficient compared to crystalline technologies. In other words, they tend to lose less of their rated capacity as temperature rises. Hence, under Singapore’s climatic condition, thin film technologies will generate 5-10% more electricity per year.

A PV module data sheet should specify the temperature coefficient

Technology	Temperature Coefficient [%/°C]
Crystalline silicon	-0.4 to -0.5
CIGS	-0.32 to -0.36
CdTe	-0.25
a-Si	-0.21



The single-line diagram of the proposed three-phase, single-stage, grid-connected PV system with a CSI as the power-conditioning unit. The PV array is a parallel combination of PV modules, while each PV module is a series combination of PV cells. The dc-side inductor filters out the ripples in the dc-side current and allows its control. The ac-side of the inverter is interfaced with the primary side of the transformer through a capacitive filter composed of three Y-connected capacitors. The function of is to absorb switching harmonics and produce clean sinusoidal current at the grid interface. Breaker is an integral part of the PV system and is provided to protect the PV system by isolating it when there is fault on the secondary side of the transformer. The primary side of the

transformer is delta-connected whereas its secondary side is star-connected with a solidly grounded neutral point. The resistance and inductance of the distribution line are represented by  $R$  and  $L$ , respectively.  $P$  and  $Q$ , respectively, represent the active and reactive powers supplied by the PV system to the distribution system. The breaker is part of the protection system installed by the utility.

The control structure proposed for the CSI-based PV system is composed of an outer current control loop designed to control the dc-side current and an inner current control loop responsible for controlling the current that is injected into the grid. A maximum power point tracker (MPPT) is employed to ensure that the PV array is operating at its maximum power.

### III. PROPOSED METHOD AND RESULTS

#### Z-SOURCE INVERTER

A **Z-source inverter** is a type of power inverter, a circuit that converts direct current to alternating current. It functions as a buck-boost inverter without making use of DC-DC Converter Bridge due to its unique circuit topology

#### TYPES OF INVERTERS

Inverters can be classified by their structure:

##### 1. Single-phase inverter:

This type of inverter consists of two legs or two poles. (A pole is connection of two IGBTs where source of one and drain of other are connected and this common point is taken out).

##### 2. three-phase inverter:

This type of inverter consists of three legs or poles or four legs (three legs for phases and one for neutral).

But, inverters are also classified based on the type of input source. And they are,

##### 1. Voltage-source inverter (VSI)

In this type of inverter, a constant voltage source acts as input to the inverter bridge. The constant voltage source is obtained by connecting a large capacitor across the DC source.

##### 2. Current-source inverter (CSI)

In this type of inverter, a constant current source acts as input to the inverter bridge. The constant current source is obtained by connecting a large inductor in series the DC source.

#### Disadvantages

Typical inverters (VSI and CSI) have few disadvantages. They are listed as,

- Behave in a boost or buck operation only. Thus the obtainable output voltage range is limited, either smaller or greater than the input voltage.
- Vulnerable to EMI noise and the devices gets damaged in either open or short circuit conditions.
- The combined system of DC-DC boost converter and the inverter has lower reliability.

- The main switching device of VSI and CSI are not interchangeable.

To overcome these disadvantages a new concept was developed in year 2002 by Dr. F.Z. Peng. This involves combination of VSI and CSI to form a cross coupled network of two inductors and two capacitors, known as Impedance Network.

#### Operation of Z-source inverter

Normally, three phase inverters have 8 vector states (6 active states and 2 zero states). But ZSI along with these 8 normal vectors has an additional state known as the shoot through state, during which the switches of one leg are short circuited. In this state, energy is stored in the impedance network and when the inverter is in its active state, the stored energy is transferred to the load, thus providing boost operation. Whereas, this shoot through state is prohibited in VSI.

To achieve the buck-boost facility in ZSI, required Pulse-width modulation is as shown in figure. The normal Sinusoidal PWM (SPWM) is generated by comparing carrier triangular wave with reference sine wave. For shoot through pulses, the carrier wave is compared with two complementary DC reference levels. These pulses are added in the SPWM, highlighted in figure. ZSI has two control freedoms: modulation of the reference wave which is the ratio of amplitude of reference wave to amplitude of carrier wave and shoot through duty ratio which can be controlled by DC level.

#### Advantages of ZSI

The advantages of Z-source inverter are listed as follows,

- The source can be either a voltage source or a current source. The DC source of a ZSI can either be a battery, a diode rectifier or a thyristor converter, a fuel cell stack or a combination of these.
- The main circuit of a ZSI can either be the traditional VSI or the traditional CSI.
- Works as a buck-boost inverter.
- The load of a ZSC can either be inductive or capacitive or another Z-Source network.

#### Applications

1. Renewable energy sources
2. Electric vehicles
3. Motor drives

### V. EFFICIENCY ANALYSIS OF QZSI MODULE

#### A. Operating State Analysis

When using the improved phase shifted sinusoidal pulse width modulation (PS-SPWM) in [17], the switch states of qZSI module can be presented in the positive half fundamental cycle, as shown in Fig. 6, because there are the same states in the negative half cycle. When comparing to the traditional H-bridge module's operating states, shoot-through states 1 and 2 are added in the qZSI module. As a result, there are five operating states in one switching cycle  $T_s$ , i.e., traditional zero states 1 and 2, shoot-through states 1 and 2, and

active state in Fig. 6, and the equivalent circuit of each operating state is shown in Fig.

As shown in Fig. 7, the devices of qZSI module have different on-state currents during one switching cycle, which affects the device power loss.

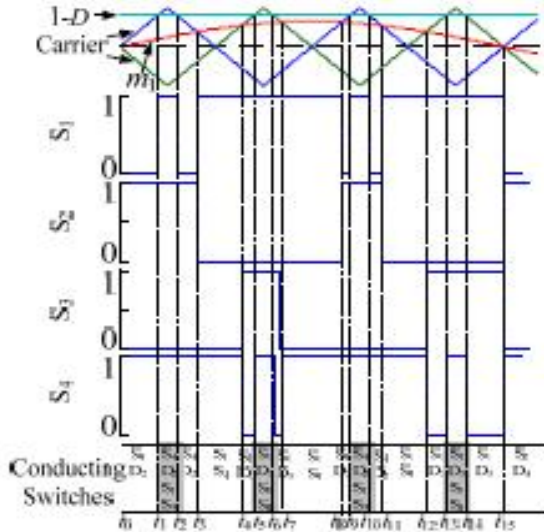


Fig.5.1. Switching states of qZSI module.

**B. Power Loss Calculation**

The qZSI module's loss includes one caused by traditional states and one caused by shoot-through states. The total loss consists of H-bridge device loss, qZS diode loss, and inductor and capacitor losses of qZS network.

**(1) H-bridge device power loss**

1) Conduction loss

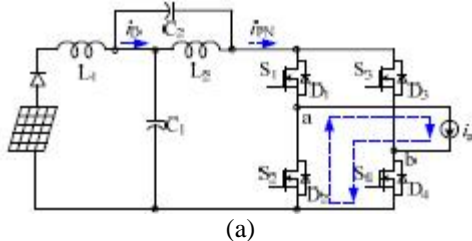
The conduction loss includes the switch loss in forward conduction and the conduction loss of the free-wheeling diode [20]. In traditional states there is

$$P_{con\_s\_tr} = \frac{2}{\pi} \int_0^\pi [R_{DS(on)} \cdot i_a^2 \cdot \frac{1+m}{2}] d\omega \tag{20}$$

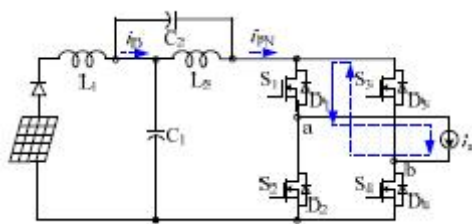
$$+ \frac{2}{\pi} \int_0^\pi [u_{D0} \cdot i_a + R_D \cdot i_a^2] \cdot (1 - \frac{1+m}{2}) d\omega$$

Where  $R_{DS(on)}$  is the drain-source on-state resistance of MOSFET.  $u_{D0}$  and  $R_D$  are the on-state zero-current voltage and the on-state resistance of the anti-parallel diode, respectively.

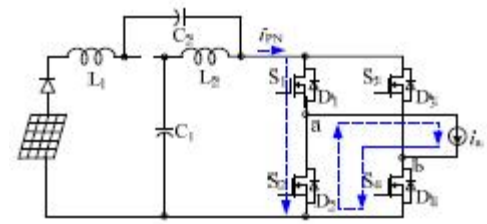
They are available in datasheet.



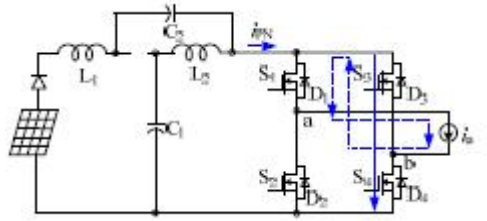
(a)



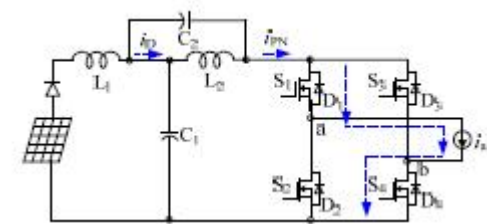
(b)



(c)



(d)



(e)

Fig.2. Equivalent circuits in one switching cycle. (a) Traditional zero state 1,  $S_{1234}=\{0\ 1\ 0\ 1\}$ ; (b) traditional zero state 2,  $S_{1234}=\{1\ 0\ 1\ 0\}$ ; (c) shoot-through state 1,  $S_{1234}=\{1\ 1\ 0\ 1\}$ ; (d) shoot-through state 2,  $S_{1234}=\{1\ 0\ 1\ 1\}$ ; (e) active state,  $S_{1234}=\{1\ 0\ 0\ 1\}$ .

The conduction loss in shoot-through states is

$$P_{con\_s\_th} = 4 \cdot [R_{DS(on)} \cdot (2i_{L1})^2 \cdot \frac{D}{2}] \tag{21}$$

2) Switching loss

The switching loss of MOSFET includes the turn on/off loss, and the reverse recovery loss of the anti-parallel diode [20].

From Fig. 6, the switching loss in traditional states is

$$P_{sw\_s\_tr} = \frac{2}{\pi} \int_0^\pi [V_{PN} \cdot i_a \cdot \frac{tri+tfu}{2} \cdot f_s] d\omega \tag{22}$$

$$+ 2 \cdot Q_{rr} \cdot V_{PN} \cdot f_s + \frac{2}{\pi} \int_0^\pi [V_{PN} \cdot i_a \cdot \frac{tru+tfi}{2} \cdot f_s] d\omega$$

Where  $tri$  is the current rise time,  $tfu$  is the voltage fall time,  $tru$  is the voltage rise time,  $tfi$  is the current fall time,  $Q_{rr}$  is the reverse recovery charge. They are available in datasheet. The switching loss in shoot-through states is

$$P_{sw\_s\_th} = 2 \cdot V_{PN} \cdot 2i_{L1} \cdot \frac{tri+tfu}{2} \cdot f_s \tag{23}$$

$$+ 2 \cdot V_{PN} \cdot 2i_{L1} \cdot \frac{tru+tfi}{2} \cdot f_s$$

**(2) QZS diode power loss**

The qZS diode power loss consists of the conduction loss and the reverse recovery loss.

The conduction loss of qZS diode is

$$P_{con\_D} = \frac{2}{\pi} \int_0^{\pi} [u_{D0\_z} \cdot 2i_{L1} + R_{D\_z} \cdot (2i_{L1})^2] \cdot (1-D-m) d\omega t + \frac{2}{\pi} \int_0^{\pi} [u_{D0\_z} \cdot (2i_{L1} - i_a) + R_{D\_z} \cdot (2i_{L1} - i_a)^2] \cdot m d\omega t \quad (24)$$

where  $u_{D0-z}$  and  $R_{D-z}$  are the on-state zero-current voltage and the on-state resistance of the qZS network diode, respectively.

The reverse recovery loss is

$$P_{rr\_D} = 2 \cdot Q_{rr\_z} \cdot V_{PN} \cdot f_s \quad (25)$$

Where  $Q_{rr-z}$  is the reverse recovery charge of the qZS diode.

**(3) QZS inductor power loss**

The inductor's loss consists of copper loss and core loss. Copper loss is expressed by

$$P_{Cu} = i_{L1}^2 R_L \quad (26)$$

Where  $R_L$  is the inductor's resistance.

Core loss is expressed by

$$P_{Fe} = pV_e \quad (27)$$

where  $V_e$  is the core volume, and  $p$  is the loss coefficient, for high flux core 58090, there is the half of AC flux swing, and  $f$  is the frequency.

So the inductor's loss is

$$P_L = 2P_{Cu} + P_{Fe} \quad (28)$$

**(4) QZS capacitor power loss**

Different operating states cause different capacitor currents, as shown in Table II. The rms value of the capacitor current is calculated as

$$I_{C1} = \sqrt{(-i_{L1})^2 \cdot D + \frac{1}{\pi} \int_0^{\pi} i_{L1}^2 \cdot (1-m-D) d\omega t + \frac{1}{\pi} \int_0^{\pi} (i_{L1} - i_a)^2 \cdot m d\omega t} \quad (29)$$

The power loss of two capacitors are expressed by

$$P_{C1C2} = 2(I_{C1})^2 R_{esr} \quad (30)$$

**VI. QZS-CMI PV POWER SYSTEM'S OPERATION**

Tests of QZS-CMI based PV system are fulfilled in the experimental setup shown in Fig. 10. The control method shown in Fig. 11 is employed, including the distributed MPPT control, the independent DC-link peak voltage control, and the grid-injected power control [17]. As shown in Fig. 6.1 (a), each PV panel is controlled to operate at the maximum power point (MPP) by regulating  $D_n$ . At the same time each DC-link peak voltage has the same value. Fig. 6.1 (b) shows the grid power control for the whole system.

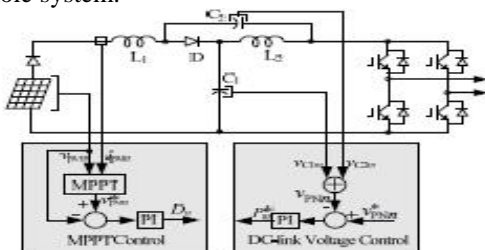


Fig. 1 (a)

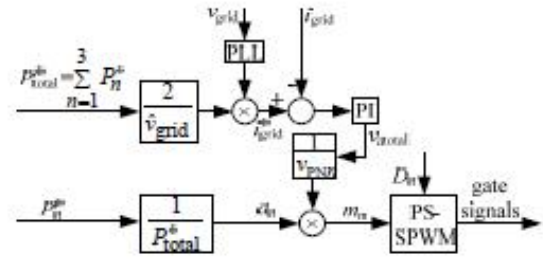


Fig. 6.1 (b)

Fig.6.1. Control scheme for QZS-CMI based PV power system. (a) Control method of each qZSI module; (b) power control of the whole system. SIMULINK MODEL

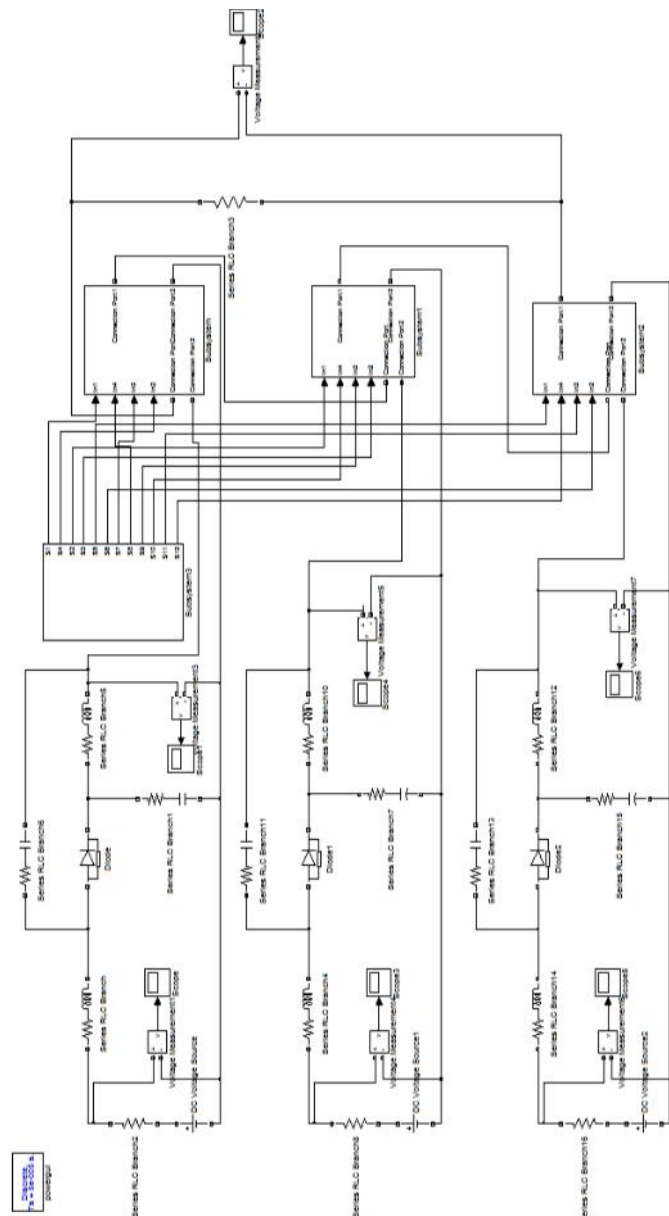


Fig.2. Quasi Z-source inverter simulation circuit

WAVEFORMS

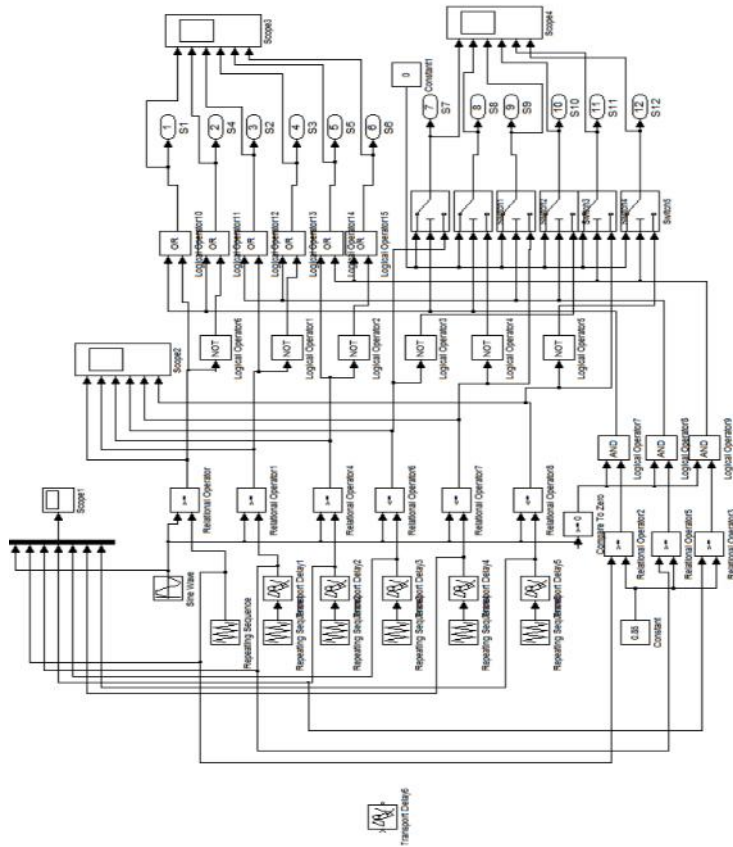


Fig.3. PWM control technique

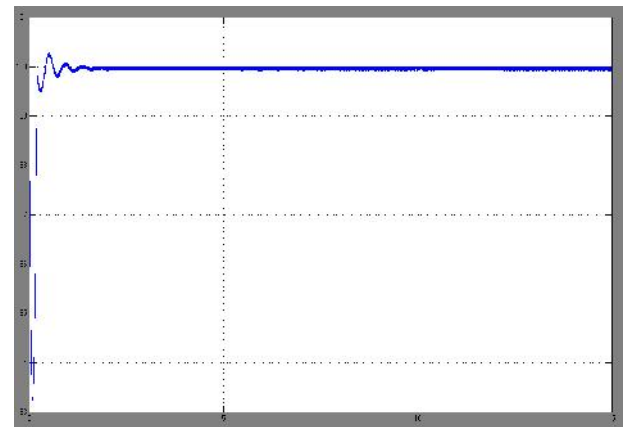


Fig5. DC link voltage

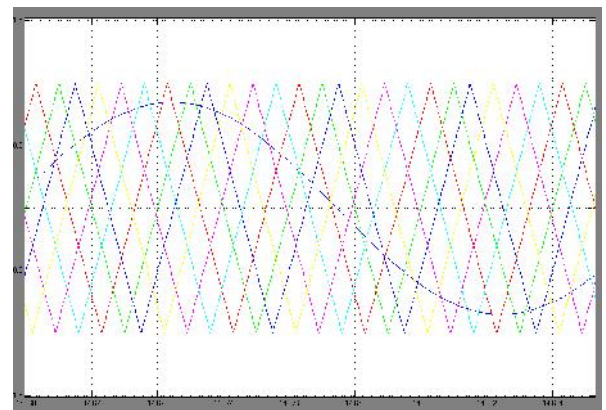


Fig.6. SPWM technique

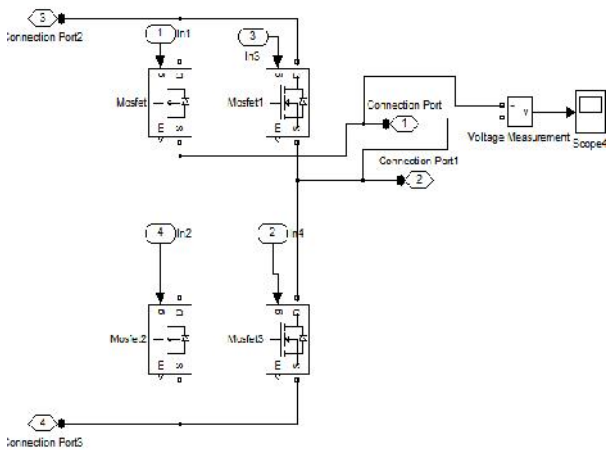


Fig.4. Inverter connection

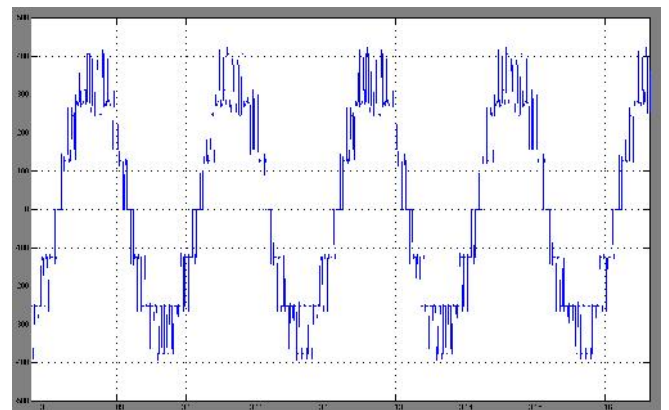


Fig.7. Seven level inverter output voltage

## CONCLUSION

This paper proposed an analytic model for the QZSI module of QZS-CMI system to address the relationship between the 2w voltage (and current) ripples and the impedance parameters. An impedance design method was proposed to limit the 2w ripples in the desired range. Simulations and experiments with different impedance parameters were carried out to verify the proposed analytic model and design method.

The efficiency calculation method was proposed to analyze this kind of QZS-CMI system. The measured efficiency and the theoretical efficiency were compared through using a designed prototype, and the identical results verified the efficiency analysis method. Finally, the experimental results of QZS-CMI based PV system validated the theoretical analysis and the system characteristics.

## REFERENCES

- [1] N.A. Rahim, M.F.M. Elias, W. P. Hew, "Transistor-clamped H-bridge based cascaded multilevel inverter with new method of capacitor voltage balancing," *IEEE Trans. Ind. Electron.*, vol.60, no.8, pp.2943-2956, Aug. 2013.
- [2] F. Filho, L. Tolbert, B. Ozpineci, and J. Pinto, "Adaptive selective harmonic minimization based on ANNs for cascade multilevel inverters with varying DC sources," *IEEE Trans. Ind. Electron.*, vol.60, no.5, pp.1955-1962, May 2013.
- [3] E. Villanueva, P. Correa, J. Rodriguez, and M. Pacas, "Control of a single-phase cascaded H-bridge multilevel inverter for grid-connected photovoltaic systems," *IEEE Trans. Ind. Electron.*, vol. 56, no. 11, pp. 4399-4406, Nov. 2009.
- [4] J. Chavarria, D. Biel, F. Guinjoan C. Meza, and J. Negroni, "Energy-balance control of PV cascaded multilevel grid-connected inverters for phase-shifted and level-shifted pulse-width modulations," *IEEE Trans. Ind. Electron.*, vol. 60, no. 1, pp. 98-111, Jan. 2013.
- [5] M. Malinowski, K. Gopakumar, J. Rodriguez, and M. A. Pérez, "A survey on cascaded multilevel inverters," *IEEE Trans. Ind. Electron.*, vol. 57, no. 7, pp. 2197-2206, Jul. 2010.
- [6] M. A. Parker, R. Li, and S.J. Finney, "Distributed control of a fault-tolerant modular multilevel inverter for direct-drive wind turbine grid interfacing," *IEEE Trans. Ind. Electron.*, vol.60, no.2, pp.509-522, Feb. 2013.
- [7] L. Liu, H. Li, Y. Zhao, X. He, and Z.J. Shen, "1 MHz cascaded Z source inverters for scalable grid-interactive photovoltaic (PV) applications using GaN device," *IEEE ECCE'2011*, Sept. 2011, pp. 2738-2745.
- [8] Y. Zhou, L. Liu, and H. Li, "A high performance photovoltaic module-integrated converter (MIC) based on cascaded quasi-z-source inverters (qZSI) using eGaN FETs," *IEEE Trans. Power Electron.* vol.28, no.6, pp. 2727-2738, Jan. 2013.
- [9] D. Sun, B. Ge, F. Z. Peng, H. Abu-Rub, D. Bi and Y. Liu, "A new grid-connected PV system based on cascaded H-bridge quasi-Z source inverter," *IEEE Intern. Symp. on ISIE*, May 2012, pp. 951-956.
- [10] B. Ge, "Energy Stored Cascade Multilevel Photovoltaic Grid-Tie Power Generation System," China Patent CN101917016A, Dec. 15 2010.
- [11] Y. Liu, B. Ge, H. Abu-Rub, F. Z. Peng, "An effective control method for quasi-Z-source cascade multilevel inverter-based grid-tie single-phase photovoltaic power system," *IEEE Trans. Ind. Informat.*, vol.10, no.1, pp.399-407, Feb. 2014.
- [12] B. Ge, H. Abu-Rub, F. Peng, Q. Lei, de Almeida A., Ferreira F., D. Sun, Y. Liu, "An energy stored quasi-Z-source inverter for application to photovoltaic power system," *IEEE Trans. Ind. Electronics*, vol.60, no.10, pp.4468-4481, Oct. 2013.
- [13] D. Vinnikov, I. Roasto, R. Strzelecki, and M. Adamowicz, "Step-up DC/DC converters with cascaded quasi-z-source network," *IEEE Trans. Ind. Electron.*, vol.59, no.10, pp.3727-3736, Oct. 2012.
- [14] Y. Li, S. Jiang, J.G. Cintron-Rivera, F. Z. Peng, "Modeling and control of quasi-Z-source inverter for distributed generation applications," *IEEE Trans. Ind. Electron.*, vol.60, no.4, pp.1532-1541, April 2013.
- [15] Y. Yu, Q. Zhang, B. Liang, and S. Cui, "Single-phase Z-source inverter: analysis and low-frequency harmonics elimination pulse width modulation," *IEEE ECCE'2011*, Sept. 2011, pp. 2260-2267.
- [16] Z. Gao, Y. Ji, Y. Sun, and J. Wang, "Suppression of voltage fluctuation on DC link voltage of Z-source," *Journal of Harbin University of Science and Technology*, vol.16, no.4, pp.86-89, Aug. 2011.
- [17] D. Sun, B. Ge, D. Bi, and F. Z. Peng, "Analysis and control of quasi-Z source inverter with battery for grid-connected PV system," *International Journal of Electrical Power & Energy Systems*, vol. 46, pp. 234-240, March 2013.
- [18] Y. Liu, B. Ge, H. Abu-Rub, F. Z. Peng, "Control system design of battery-assisted quasi-Z-source inverter for grid-tie photovoltaic power generation," *IEEE Trans. Sustain. Energy*, vol.4, no.4, pp.994-1001, Oct. 2013.
- [19] Y. Liu, B. Ge, H. Abu-Rub, F.Z. Peng, "Overview of space vector modulations for three-phase Z-source/quasi-Z-source inverters," *IEEE Trans. Power Electron.*, vol.29, no.4, pp.2098-2108, April 2014.
- [20] D. Graovac, M.Purschel, and A.Kiep, "MOSFET power losses calculation using the data-sheet parameters," *Automotive Power, Application Note*, vol.1.1, Jul. 2006.